



# Molecular depth profiling and imaging using cluster ion beams with femtosecond laser postionization

D. Willingham\*, A. Kucher, N. Winograd

Department of Chemistry, Pennsylvania State University, University Park, PA 16802, United States

## ARTICLE INFO

### Article history:

Available online 13 May 2008

### Keywords:

Laser postionization  
C<sub>60</sub>  
Depth profiling  
3D imaging

## ABSTRACT

The emergence of cluster ion sources as viable SIMS probes has opened new possibilities for detection of neutral molecules by laser postionization. Previous studies have shown that with atomic bombardment multiphoton ionization using high-power femtosecond pulses leads to photofragmentation. The large amount of photofragmentation can be mostly attributed to high amounts of internal energy imparted to the sputtered molecules during the desorption process. Several pieces of preliminary data suggest that molecules subjected to cluster beam bombardment are desorbed with lower internal energies than those subjected to atomic beam bombardment. Lower energy molecules may then be less likely to photodissociate creating less photofragments in the laser postionization spectra. Here we present data taken from coronene films prepared by physical vapor deposition comparing a 40 keV C<sub>60</sub><sup>+</sup> ion source with a 20 keV Au<sup>+</sup> ion source, which supports this hypothesis. Furthermore, the depth profiling capabilities of cluster beams may be combined with laser postionization to obtain molecular depth profiles by monitoring the neutral flux. In addition, imaging and depth profiling may be combined with atomic force microscopy (AFM) to provide three-dimensional molecular images.

© 2008 Elsevier B.V. All rights reserved.

## 1. Introduction

Laser postionization in secondary neutral mass spectrometry (LPI-SNMS) has been shown to increase the ionization of atomic species produced by ion bombardment resulting in mass selected images superior to those produced by traditional time of flight secondary ion mass spectrometry (ToF-SIMS). LPI-SNMS is, however, much less successful when dealing with molecular species. Most molecular species exhibit a great deal of photofragmentation when introduced to the femtosecond laser beam. The extent of photofragmentation present when analyzing molecular species is attributed to the large amount of internal energy imparted to the molecules during the sputtering process [1].

Several pieces of preliminary data, including data presented in this paper, suggest that the use of a C<sub>60</sub> primary ion beam in place of the traditional liquid metal ion guns (LMIGs) results in desorbed neutral molecules with lower internal energies [2]. Consequently, the combination of the C<sub>60</sub> primary ion beam with LPI may be capable of producing sufficient amounts of molecular ions in order to achieve LPI molecular depth profiles. Of particular importance is the ability to compare these LPI depth profiles to traditional ToF-SIMS

depth profiles for the purpose of isolating the sputtering physics from ionization effects present in the surface and interface regions of the sample. In addition, the LPI profiling capability presented in this paper may be combined with already existing LPI imaging capabilities aimed at achieving LPI three-dimensional images.

## 2. Experimental

The experiments were performed in a ToF-SIMS apparatus equipped with a 40 keV C<sub>60</sub> source, a 25 keV Au source, cryogenic cooling capabilities, and calcium fluoride (CaF<sub>2</sub>) windows for integration with a femtosecond titanium sapphire chirped pulse amplification (CPA) laser system described in detail elsewhere [3]. Under typical operating conditions, the CPA laser system produces 200-fs light pulses at a wavelength of 800 nm and an average power of 1.5 mJ at a 1-kHz repetition rate. The laser light pulses are integrated into the typical SIMS experiment by exact control of timings between the light pulse, the primary ion pulse, a suppression pulse to reduce secondary ions produced during sputtering, and the extraction pulse required to push the LPI ions into the mass analyzer. The experimental setup is identical to the LMIG postionization experiment published previously except for the addition of a time delay box designed to accommodate the longer flight times of the 40 keV C<sub>60</sub> ions. The LPI spectra for the C<sub>60</sub> and Au projectiles were acquired at liquid nitrogen temperatures

\* Corresponding author.

E-mail address: [dgw140@psu.edu](mailto:dgw140@psu.edu) (D. Willingham).

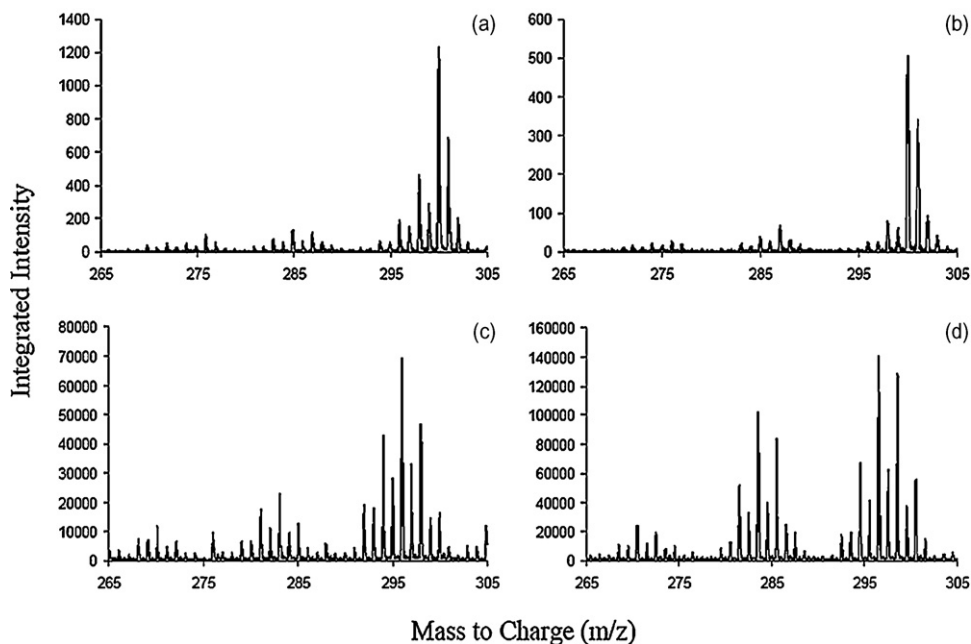


Fig. 1. (a) High mass portion ( $m/z$  265–305) of SIMS coronene spectra using 40 keV  $C_{60}$  source; (b) SIMS 20 keV Au source; (c) LPI 40 keV  $C_{60}$  source; (d) LPI 20 keV Au source.

to minimize thermal fragmentation and reduce interference from volatile species. These positive ion mass spectra were obtained during the data acquisition cycles by digitizing the analog signal with a transient digitizer (TD; PDA500, Signatec). For comparison, SIMS spectra for the two projectiles were acquired under identical conditions using a time to digital converter (TDC; 98063 PCI, Precision Instruments Inc.) data acquisition card. The LPI images were obtained by rastering the  $C_{60}$  primary ion beam across the sample at a field of view (FOV) of approximately  $300 \mu\text{m} \times 300 \mu\text{m}$ . The LPI depth profiling experiments were carried out by alternating between sputter erosion cycles and data acquisition cycles in the presence of the femtosecond laser pulses. The ion intensities obtained from these experiments were normalized to total counts and plotted as a function of primary ion fluence.

Coronene (Aldrich Chemical Co.) thin films are prepared in a modified stainless steel physical vapor deposition (PVD) chamber [4]. During the PVD process a crucible containing 500 mg of coronene powder is heated resistively by passing approximately 15 A through a tungsten filament. Coronene gas sublimates out of the reservoir at approximately  $200^\circ\text{C}$ , passes through a defusing grid, and deposits on pre-cut silicon shards (Ted Pella Inc.) cooled to liquid nitrogen temperature. The coronene films are deposited with a thickness of 200–400 nm depending on deposition rate and temperature. The film thickness is monitored by a quartz crystal microbalance (QCM; TM-400, Mextek Inc.) and validated using atomic force microscopy (AFM; Nanopics 2100, TLA Tencor Inc.). For imaging purposes, it is necessary to perform a simple lithography technique whereby a 400 mesh London finder grid (Electron Microscopy Sciences) is placed over the silicon shard prior to deposition and then removed once the deposition has subsided. This masking technique results in a coronene thin film containing a relief pattern of the grid bars and characters. AFM data show that the edge definition between the coronene film and the silicon is approximately  $2 \mu\text{m}$ . The root mean square roughness of the film is 8 nm, as determined by an AFM measurement over an area of  $20 \mu\text{m}^2$ .

### 3. Results and discussion

The spectra shown in Fig. 1 compare the SIMS and LPI spectra taken with the  $C_{60}$  and Au ion sources. It is logical for the LPI spectra to contain higher amounts of fragmentation due to previously described photodissociation; however, it is of greater importance to compare the two LPI spectra and the two SIMS spectra, respectively. Typically mass to fragment (M/F) ratios obtained by dividing the molecular ion intensity by the fragment ion intensities provide the most insight into the extent of LPI fragmentation. It is evident from the M/F ratios for the high mass fragments shown in Fig. 1 that the  $C_{60}$  LPI spectra contains more hydrogen ( $H_n$ ) loss fragments than carbon ( $C_nH_n$ ) loss fragments. The LPI spectrum for Au primary ions also contains a significant number of  $H_n$ -loss fragments; however, there is more fragmentation of the molecular ion through  $C_nH_n$ -loss than is observed for  $C_{60}$  primary ions. This trend is also present in the SIMS spectra, although to a much lesser extent. These observations may be explained by exploring previously described fragmentation pathways of polyaromatic hydrocarbons (PAHs) [5]. It has been shown that PAHs such as coronene dissociate by the aforementioned fragmentation pathways;  $H_n$ -loss and  $C_nH_n$ -loss. Experimental evidence reported earlier suggests that neutral molecules with higher internal energies will tend to dissociate by the  $C_nH_n$ -loss fragmentation pathway, whereas neutral molecules with lower internal energies dissociate by the  $H_n$ -loss fragmentation pathway [6]. The data presented in Fig. 1 support the hypothesis that neutral molecules sputtered by the  $C_{60}$  primary beam have lower internal energies and therefore show more  $H_n$ -loss fragments than those sputtered by Au primary ions, which show more  $C_nH_n$ -loss fragments. Previous work examining the LPI of silver monomers and dimers sputtered by  $C_{60}$  shows that the ejection mechanism resembles a jet-like expansion of a plume of super-heated and super-dense gas [7]. The data presented here, in conjunction with prior research, suggest that not only does  $C_{60}$  produce a higher yield of secondary neutral molecules, but also a higher yield of intact molecular species. It is important to note that the variations in intensities represented in Fig. 1 are a direct result of differences

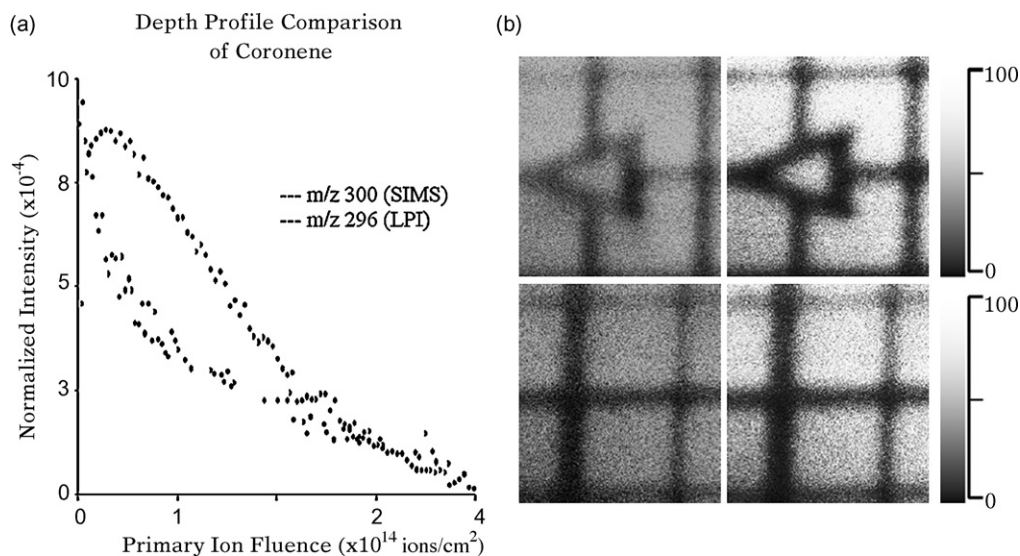


**Fig. 2.** (a) SIMS and LPI molecular ion signals obtained by depth profiling a 200 nm coronene film; (b) Images of coronene patterned films; total ion images (right) and coronene (light grey)/silver (dark grey) ions distributions (left) in a 125  $\mu\text{m} \times 125 \mu\text{m}$  field of view obtained by LPI using a  $\text{C}_{60}$  primary ion source.

in the data acquisition between the LPI (TD) and SIMS (TDC) spectra. The TD acquisition was employed in the LPI experiments due to the presence of multiple ion events at each binning point. After compensating for the data acquisition differences, the LPI signal for the coronene molecular ion is on the same order as that observed by SIMS.

Hence, it is feasible to perform molecular depth profiling experiments by monitoring both the secondary ion intensity and the secondary neutral molecule intensity. This comparison is shown in Fig. 2a for a coronene film deposition onto silver foil. The LPI molecular ion signal as a function of primary ion fluence starts at a maximum value and declines in an exponential fashion. On the other hand, the SIMS molecular ion signal first increases and then decreases with increased fluence. It is hypothesized that this behavior results from two competing effects. The first effect arises from the formation of molecular damage, which appears in the LPI depth profile. Because the LPI signal is not dependent on surface ionization effects, the molecular damage profile is seen quite well. The second effect involves changes in the ionization probability with fluence, either due to the removal of surface contaminants or the buildup of protons as a consequence of the  $\text{C}_{60}$  bombardment. The SIMS depth profile is a convolution of both the surface ionization effects resulting in the observed maximum intensity at non-zero fluence. Signals from the silver–coronene interface were not observed due to the roughness of the silver foil (Aldrich Chemical Co.). These effects will be interesting to study in the future using a more appropriate substrate.

In addition to the LPI depth profiling of coronene films, it is of interest to examine the imaging capability of this approach. The total ion and mass selected images obtained from patterned coronene films on a vapor deposited silver (Aldrich Chemical Co.) substrate are shown in Fig. 2b. Topographical differences in the films are clearly observed in the total ion images where the relief pattern of the film is raised approximately 200 nm from the silver substrate. The top images are of a character located within the London funder grid and the bottom images are of an area containing only grid bars. It is clear that the LPI  $\text{C}_{60}$  imaging capabilities

integrate well with the patterned coronene films as a proof of concept. It is, therefore, the next logical step to combine the profiling capabilities with LPI  $\text{C}_{60}$  imaging in order to realize three-dimensional LPI  $\text{C}_{60}$  images by a previously described protocol [8].

#### 4. Conclusion

In summary, the goal of this research has been to show the efficacy of combining LPI with a  $\text{C}_{60}$  primary ion SIMS source for imaging and depth profiling capabilities. The data presented in this paper suggest that neutral molecules sputtered by  $\text{C}_{60}$  are, indeed, cooler than those sputtered by Au. This result further supports the prospect of using  $\text{C}_{60}$  to increase secondary ion yields of intact molecular ions. In the future, it is a goal of this research to evaluate the efficacy of using  $\text{C}_{60}$  LPI to ionize a wider range of biological molecules such as lipids, amino acids, and saturated organics. Moreover, the depth profiling and imaging capabilities of  $\text{C}_{60}$  LPI have been explored using coronene thin films created by PVD as a model system. It is, therefore, conceivable that the depth profiling and imaging capabilities established in this paper may be combined in order to obtain three-dimensional LPI images.

#### Acknowledgements

The authors acknowledge the Department of Energy under grant #DE-FG02-06ER15803 and the National Science Foundation grant #CHE-555314 for partial financial support of this research.

#### References

- [1] V. Vorsa, et al. *Anal. Chem.* 71 (1999) 574.
- [2] A. Wucher, et al. *Anal. Chem.* 76 (2004) 7234–7242.
- [3] K.F. Willey, V. Vorsa, R.M. Braun, N. Winograd, *Rapid Commun. Mass Spec.* 12 (1998) 1253.
- [4] Z. Zhu, D.L. Allara, N. Winograd, *Appl. Surf. Sci.* 252 (2006) 6686–6688.
- [5] S.J. Pachuta, et al. *J. Am. Chem. Soc.* 110 (1988) 657.
- [6] H. Kühlewind, A. Kiermeier, H.J. Neusser, *J. Chem. Phys.* 85 (1986) 4427.
- [7] S. Sun, C. Szakal, N. Winograd, *J. Am. Soc. Mass Spectromet.* 16 (2005) 1676–1677.
- [8] A. Wucher, J. Cheng, N. Winograd, *Anal. Chem.* 79 (2007) 5529–5539.